

Design and Dynamic Analysis of a 2 Dual Axes Solar Tracking Mechanism

BEKIR CIRAK

Engineering Faculty, Mechanical Engineering Department
Karamanoglu Mehmetbey University
70100, Yunus Emre Kampus Karaman,
TURKEY

Abstract: - This paper describes the implementation of general multibody system dynamics on sun tracker mechanism. In this study, a dual axes solar tracking mechanism designed within the scope of a project to obtain an efficient electrical energy from solar rays is examined. Dynamic and kinematic calculations of the moving and joint places in the mechanism were made. This study is important as the use of an efficient solar tracker is very useful in military, industrial and residential areas. Free Body Diagrams of all the elements or limbs that make up the sun tracker mechanism have been drawn. Thus, dynamic and kinematic values at elements points were calculated. The proposed dynamics model of the mechanism offers an accurate and fast method to analyze the dynamics of the mechanism knowing that there is no suchwork available for sun tracker. Also, 3D tracker elements were drawn and planned in Solid Work program. The simulation gives a clear idea about energy parameters for different link lengths of the mechanism over a linear displacement.

Key-words: - Sun tracker, Mechanism, Dynamic, Dual Axes, Analyse.

Received: September 9, 2021. Revised: October 15, 2022. Accepted: November 12, 2022. Published: December 5, 2022.

1 Introduction

There is a great need for renewable energy and green energy in today's life. It is necessary to inherit a sustainable energy source to future people. At the same time, it is necessary to have a sustainable energy market in the future. Green energy has shown a sustainable trend. Electricity is required to relieve our homes and our daily life. Mains electricity requires great investment. It has to operate and operate large power plants. It costs a lot of money for that. is needed. To produce this energy, we need to spend a lot of time with green energy to turn to alternative energy sources and bring them to consumers such as industry, military and residences.

For military needs in the future, it is inevitable to turn to renewable energy sources that require less maintenance and are more efficient. To run a military facility, large generators are required that are not efficient and consume excessive amounts of fuel. Therefore, renewable energy is important for these facilities. Solar energy is one of them. Solar energy will be used not only for military facilities but also for mobile military units, which will be more efficient in providing energy to soldiers' equipment used in the field, [1].

In general, strictly dependence on fossil fuels is politically, economically and naturally dangerous.

Politically, the country should not be dependent on oil from other countries.

2 Tracking System

A solar tracker can increase the efficiency of a solar panel by up to 100%. It does this by always keeping the panel perpendicular to incoming sunlight rays. The main purpose of the sun tracking need is hidden here. While solar tracking is not a new concept, it is quite a new concept compared to fixed PV cells. price, efficiency, reliability, etc. half a century ago. There are a wide range of solar tracking system studies that vary in terms of In designing a solar tracking system, the system needs to maximize the output from tracking. Sometimes, the solar tracking system may not be able to match the performance of a well-positioned fixed PV panel. To compensate for this, it always keeps the panel perpendicular to incoming sunlight rays.

Although the purpose of solar monitoring is to provide more power output than a stationary PV panel, this is not always ideal. Due to the increased cost of solar tracking technology compared to fixed PV panels, solar monitoring is not always the best option. If a fixed PV panel is used, it is placed positionally facing the sun. The PV panel placement is that it should be at a point where it

will have a clear viewing angle and should be positioned at an angle facing the equator. Fixed PV panels are a cheaper energy solution, but do not fully utilize the energy from the sun, [2].

2.1 Active Tracking

It uses motors, gears, and actuators to position the solar tracker perpendicular to the sunlight. Using sensors to track the sun position, the solar tracking system sends data to the controller, driving the motors and actuators to position the panel (collector). There is also a tracking system that uses the sun chart. Solar charts provide information on the position of the sun at different times of the day throughout the year, depending on location. In the tracking system that uses the sun chart, there is no need for a sensor to track the sun. However, there is a tracking system that uses both the sensor and the sun chart. The sensor is used in sunny weather for tracking the sun. However, during cloud-covered times, information from the sun chart is used. Since the solar tracking system can generate energy even in cloudy conditions, it has become important to monitor the sun in cloudy conditions. This is certain, especially in spherical lenses, [3].

2.2 Passive Tracking

If compressed gas is used to move the solar tracking system, it is called passive trackers. Depending on the gas containers and the position where daylight falls, a difference occurs in the gas pressure and the tracking system is moved until it reaches the equilibrium position. The advantage of the passive tracker is that the monitoring system does not require a controller. But passive viewers are slow in response and vulnerable to winds, [3].

3 Mechanics of Tracking System

If the mechanic elements are defined in general in 2 dual sun tracking system, there are 2 units as a motor that creates horizontal motion and an engine that creates vertical motion. There is a moving screw that transmits the movement of these motors to the panel frame, spur gears that rotate the frame body to the right or left. The vertical gears are provided by the moving screw. The horizontal movement is provided by the spur gears. Reducers provide the speed or rotation speed of the motors. the gears deafen it, [4].

3.1 Slewing Drive

The rotational motion in the solar tracking system enables the worm gear drive mechanism to generate

torque for rotation. They can also be found in many systems such as wind turbines, cranes, and telescopes. Worm gear mechanisms are mostly used for vertical movement in solar tracking systems. These are called single-axis drive mechanisms. If these mechanisms become worn, they become locked and cannot be rotated. This ensures that the rotary motion is resistant to wind and other external forces on the tracking system. A worm gear mechanism can be made by combining gears, bearings, seals, housing and other components in a single unit and dual unit. This mechanisms are shown in Fig. 1.a. and Fig.1.b [4].



Fig. 1.a: Single axis slewing drive

Fig. 1.b: Dual axis slewing drive

The need for a dual axis solar tracking system is in direct proportion to the ever-increasing need for solar energy. Two motors and two rotary motion elements can be operated on the same floor. In a dual axis solar tracking system, it can make both horizontal and vertical turns with a single drive system. Dual-dial drives are commonly used in solar power plants, but smaller double-turn drives are also available for the enclosures shown in Figure 2. There are also slewing drives that use spur gear instead of worm gear to achieve rotational motion. A motor connected to a small spur gear (Normal tooth, profile gear, or spur gear profile gear) is mounted vertically and as the motor rotates it rotates itself against the teeth of a spur gear fixed sprocket. Both inner and outer ring gears

can be used for this design. As this type is not self-locking, the motor must have another locking mechanism to be able to withstand external forces. This situation is illustrated in Figure 2, [5].



Fig. 2: Spur gear driven slewing drive, [4]

3.2 Linear Actuator

Elements that create motion along a straight line are called linear actuators. linear actuators, hydraulic, pneumatic, mechanical, etc. are divided into types. The most used is the mechanical linear actuator. To create a linear motion, they rotate the screw and use a screw and an electric motor for this. Linear actuators using Acme screws are self-locking compared to ball screws. Some linear actuators have a variable resistance inside, whose value varies depending on the position of the stroke. This resistor can be used to receive feedback data on the position of the stroke. Figure 3 shows a linear actuator with Acme screw and parts of it, [6].



Fig. 3: Linear actuator, [6]

The stroke (amount of thrust) and horizontal rotation of the screw can be achieved by mounting the linear actuator on an follower frame. Linear actuators with variable stroke length and gear ratio (determining the maximum thrust) can be purchased. In most cases, both a linear actuator and a slew drive are used to achieve dualaxes tracking. Linear actuators are mostly used in residential buildings because they are easy to control and inexpensive.

3.2.1 Efficiency

Compared to the fixed solar system, the efficiency of the Dualaxes PV solar system is 20-35 % under ideal conditions, while Mousazadeh et al. He found that sun tracking under ideal conditions could potentially double efficiency. With the changes of sunlight caused by the earth's rotation and cloud cover, the average electrical power that can be obtained over a year will be about 20 % of the peak wattage. Another article published in Jordan reported up to 43.87 % increases in power gain in Dualaxes tracking compared to 15.69 % for North-South tracking. Although solar cells can last between 20 and 25 years, it is reported that output power decreases by about 0.5 percent per year even with periodic maintenance to maintain the highest efficiency. This means that by the end of 20 years, they will only produce a maximum of 80 percent of their rated capacity, which is only 16 % of their peak wattage under ideal conditions.

3.2.2 Reliability

The fact that each solar panel is independent is one of the biggest advantages of converting solar energy into electricity by photovoltaic methods. Other advantages are that in the case of a faulty panel it is individually fused so that it does not affect other panels and parts can be easily replaced without affecting the entire connected system. Despite the long-term benefits of solar energy, the biggest problem is its low energy production and energy storage capability, [7].

3.2.3 Feasibility

The primary concern for investing in solar power generation is the time required for subsidies to stay in place for these systems to be autonomously profitable and viable. The fact that the price point of grid parity depends on a number of variables such as the amount of sunlight an area receives, the direction of the solar array, whether solar panels are fixed or tracking the sun, construction costs, rate structure, and financing, the options differ by more than a factor of 10 in breakeven costs. caused. Still,

grid inequality has been reached in Hawaii, where there is an average price for electricity. Arizona is another location that receives plenty of sunlight and could achieve grid parity without limited transmission access and low electricity prices. Despite these economic factors as well as practical concerns, solar energy can become the most important power source if technology grows to increase the efficiency of the system. This means that by the end of 20 years, they will only produce a maximum of 80 percent of their nominal capacity, which is only 16 % of their peak wattage under ideal conditions, [7].

4 Design

STS 444 (Stainless Steels - Special 444) material is used in the tracer metal construction. The reason why stainless is preferred is that it is resistant to corrosion, oxidation and rust in the external environment. It also has the following features.

1. Audience construction consists of panel, frame support and legs.
3. The viewer can be assembled and disassembled in a short time and easily carried.
4. Its total weight is 27 kg.
5. The vertical rotation angle of the panel is 360°.
6. The horizontal rotation angle of the panel is 180°.
7. The system is resistant to winter and summer conditions at the level of ± 50 . It has a tolerance to follow the sun at $\pm 5^\circ$. It has been fixed to the ground firmly in very windy and stormy weather.
8. The energy capacity of the viewer is 110 V. Then it can be converted to 220 V with a converter.
9. LDR sensors are designed to operate under wind and sun conditions.

The parts that make up the 10th audience have the feature to be found in the market easily and cheaply, and the necessary parts replacement in periodic repairs and maintenance can be done quickly.

12. Periodic maintenance of the monitor will be done. It will be controlled by experts.

13. There is no welding in the moving part. It does not contain any joints other than fasteners, [8].

4.1 Linkages

A four-rod connection with a linear actuator is the most commonly used connection type for elevation angle changes in the PV panel. Link 4 and Link 2 are rotated towards the ground, while Link 2 and Link 3 are connected by a frictionless slider. Link 2 is the input link and operates at a constant speed.

With this movement, the total length of the limbs 2 and 3 decreases, and Link 4 is rotated clockwise on the ground at a maximum angle of 80°. Fig.4. shows the connection of the linear actuator to the panel. It also defines the conduction angle (μ), the connections of links 1 and 4, [8].

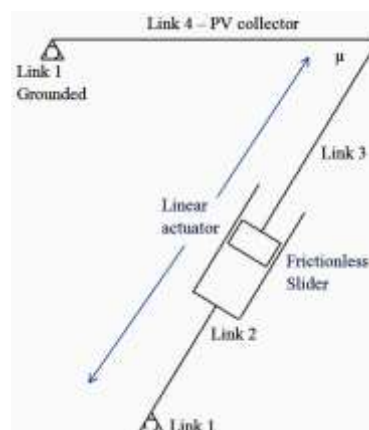


Fig. 4: Linkage of PV Elements

4.2 Linear Actuator Positioning

As the location of the connection points, Linear actuator depends on the parameters of the linear actuator size and stroke length, maximum inclination angle and transmission angle. With analytical and graphical methods, the position of the linear actuator can be calculated. Ideally, the linear actuator is pushed from an inclined position to a horizontal position while carrying the highest load, while the linear actuator will be strained. Micro voids and shear stress in the metal material structure of the tracer, decrease in the ability of the material to be exposed to stress occur in fragile materials. Although the sudden rupture in the solar tracking system designed here is unlikely to cause any damage, the creep ability and property of the STS 444 material is worrisome in terms of failure. It is an important precaution not to release the linear actuator and keep it pressed. The linear actuator has a speed of 0.05 m/s and a weight of 3560 N. The longer its stroke capacity, the heavier the linear actuator. Maximum force and tension are safe over the maximum length of the linear actuator. Connection ranges are $x \leq r = 0.40$ m and $y \leq H = 0.68$ m.

4.2.1 Position-1

The 1. positioning of the sun tracking system is the horizontal position of the panel. The angle between the X axis and the Y axis is 90°. However, the linear actuator was placed to the left of the rotating O-center. This situation is shown in Figure 5.

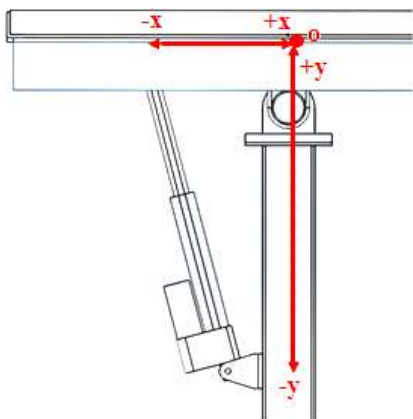


Fig. 5: 1.Positioning iteration of sun tracker

X=1-50 between value for,

$$y_a(x) = 18.24 / x$$

$$y_b(x) = 47.52 / x$$

$$y_c(x) = 88.72 / x$$

$$y_d(x) = 141.94 / x$$

$$y_e(x) = 209.74 / x$$

$$y_f(x) = 284.33 / x$$

Here, the distance y corresponding to the distance x was calculated and the curve in Fig.6 was obtained. x values (decreased / increased) or (increased / decreased) relative to that O point of the sun tracker.

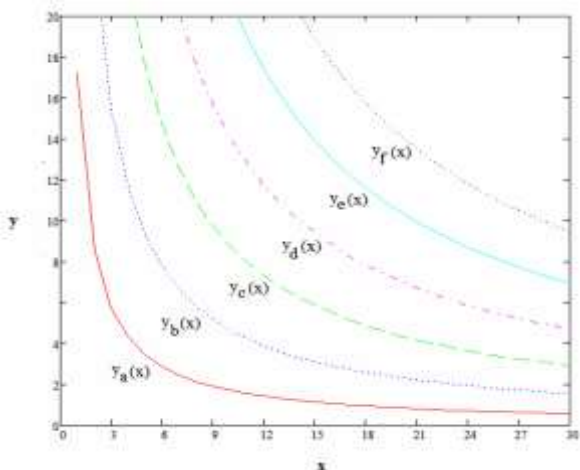


Fig. 6: x-y distances of sun tracker

The position limit on the observer body is taken so that the dimensional calculations and dynamic movements are neglected, and the connection points of the linear actuator and frame are located on the middle axis of the panel. If the pivot point (point of balance axis) is down, the optimum position of the connection points may not be on the vertical and horizontal axis.

4.2.2 Position-2

The 2.positioning of the sun tracking system is the horizontal position of the panel. The angle between the x axis and the y axis is 90°. However, the linear actuator is placed to the right of that center. This situation is shown in Figure 7.

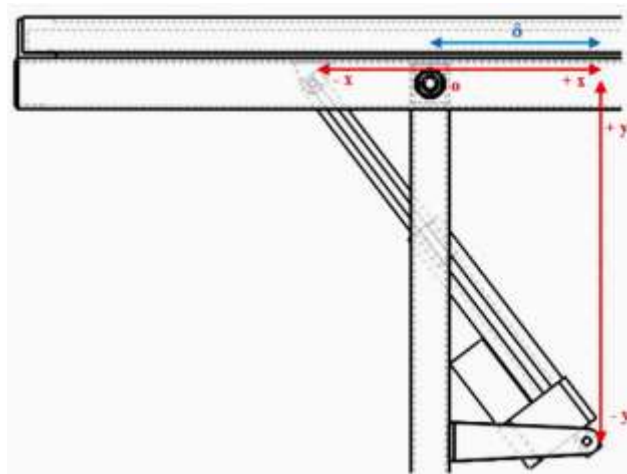


Fig. 7: 2. Position iteration of sun tracker

Two possible solutions, checked graphically for each linear actuator length, were made by the Analytical method. Transfer angles were compared for both solutions. Panel parameters are as defined in Table 1, with the panel's maximum inclination from horizontal to 80°.

Table 1. Parameters of the linear actuator, [9]

Parameter	Description
x	The horizontal distance of the linear actuator from the lower point to the upper connection points when extended maximum
y	The vertical distance of the linear actuator from the lower point to the upper connection points when extended maximum
a	Elongated length (Maximum length) of linear actuator
b	Retracted length (Minimum length) of linear actuator
l	Stroke length of linear actuator (b-a)
θ	Angle of the panel to the vertical axis
δ	Distance of linear actuator connection point to frame shaft
D	worm gear diameter in slewing driver
d	Distance between worm center and worm gear center in slewing driver
Zb	The distance between two vertical supports in the tracker's frame

Figure 8. shows the defined variants of the panel leg assembly in the two end positions defined by

the angle, extended a, retracted length b, stroke length l and offset distance δ .

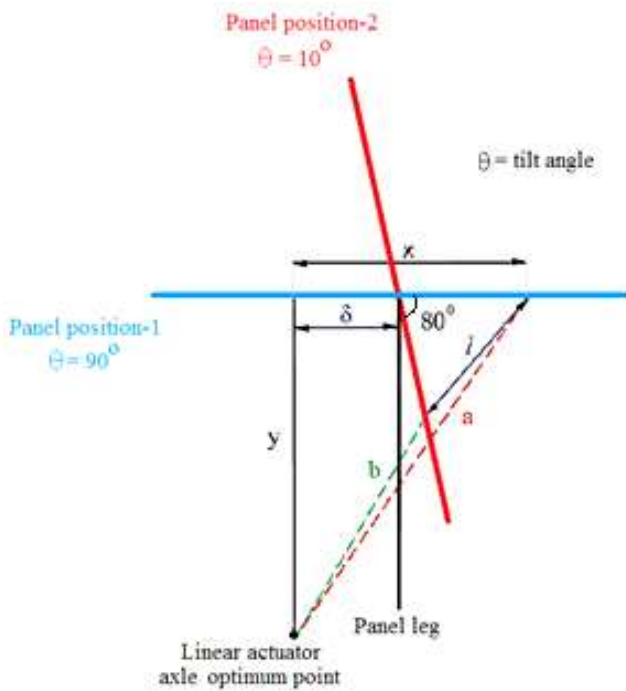


Fig. 8: 2. Position iteration of sun tracker and geometry

Depending on the stroke length l, the offset distance δ is calculated by equation (1).

$$l^2 = 2(x-\delta)^2 - 2(x-\delta) \cos 80 \tag{1}$$

Two solutions x_1 / y_1 and x_2 / y_2 are obtained from equations (2) and (3),

$$x^2 + y^2 = a^2 \tag{2}$$

$$[\delta + (x - \delta) \cos 10]^2 + [y - (x - \delta) \sin 10]^2 = b^2 \tag{3}$$

Where, a linear actuator with a stroke length of 150 mm was chosen because of its compactness and a minimum transmission angle of more than 40o.

$$a=11,69 \quad b=17,59 \quad x= 0.1 \dots\dots 20$$

$$y_a(x) = \frac{b^2 - a^2 - 2\sqrt{(b^2 - x^2)} (4,59 \sin(10)) + 4,59^2 \cos(10) - 1)2 + (4,59 \sin(10))^2}{-2,459(\cos(10) - 1)}$$

$$y_b(x) = \frac{b^2 - a^2 - 2\sqrt{(b^2 - x^2)} (4,59 \sin(10)) + 4,59^2 \cos(10) - 1)2 + (4,59 \sin(10))^2}{-2,459(\cos(10) - 1)}$$

$$y_c(x) = x$$

$$y_a(16,57) = 16,569$$

$$y_b(10,69) = 10,69$$

This state, shown in Fig 9.

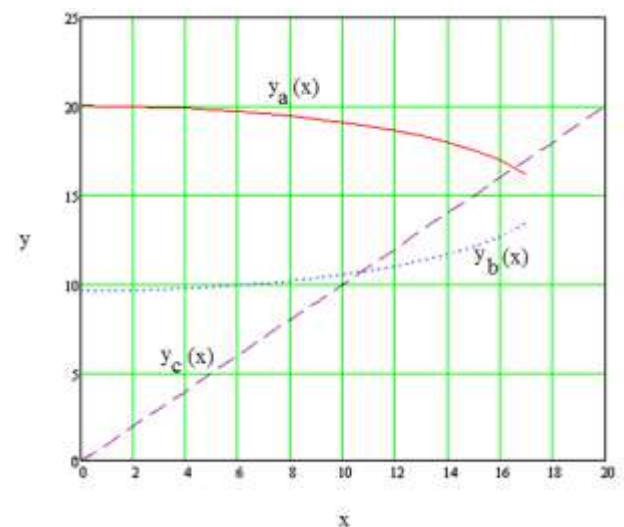


Fig. 9: x-y distances of sun tracker

In the graphic method, the linear actuator for the stroke length is 11.69 mm for min -80° and max. It is 17.59 mm for 0°. For 43,3° the optimal 0° values are valid. These values are shown in Figure 10.

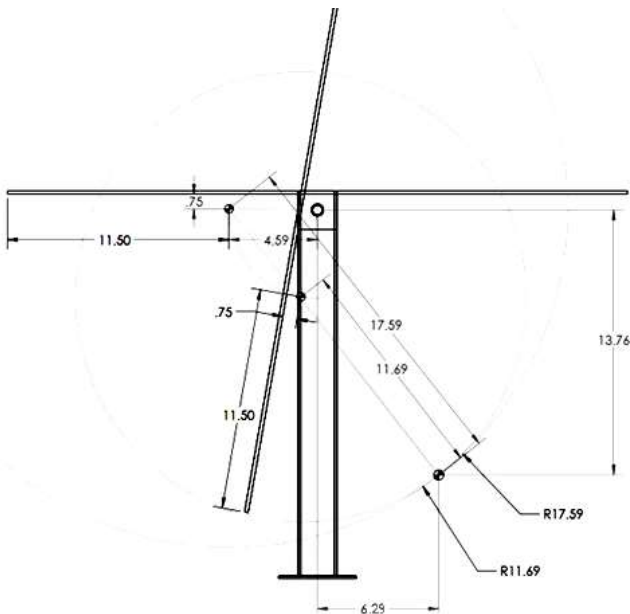


Fig. 10: Graphical method of sun tracker and geometry

The two analytical solutions obtained for the linear actuator with a stroke length of 150 mm were plotted and the corresponding transmission angles μ were measured at each location. A radius of 117 mm was drawn on the horizontal panel extending 800 to the panel tilted at this angle. With a stroke length of 272 mm x 355 mm x 127 mm respectively, the minimum transmission angle is 52° compared to a 10° transmission angle in the second position. The closer the center of gravity of the tracker's frame to the center of gravity of the linear actuator, the more stable the mount will be, requiring a smaller surface area for the base. The second solution for x and y would result in a difference of n distance from the two centers of gravity causing instability in addition to the angular momentum from the moving parts.

4.2.3 Position-3

Shown in Figure 11 is a drawing of the six-bar mechanism where the follower panel is four bars in blue and the linear actuator is divided into four bars and two four bars.

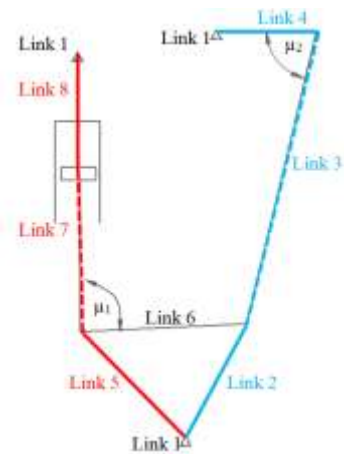


Fig. 11: Six bar mechanism

In this iteration, it consists of a Sixbar link that can be split into two Fourbar mechanisms connected by a triple link. To determine the lengths, first the Fourbar mechanism PV Fourbar on the right (Figure 11 blue) can be studied through the Connections program by varying the amount of lengths, bearing in mind that the transmission angle is greater than 40° minimum.

In gear analysis, the gear mechanism type is internal spur gear and road curved curve. This gear mechanism for 180° movement of the tracer base. This situation is shown in Figure 12.

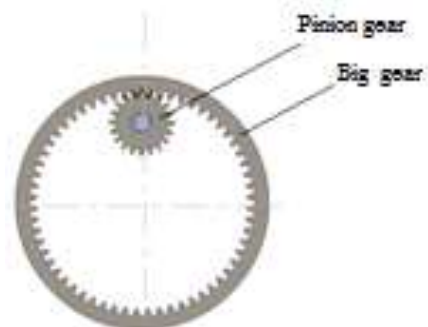
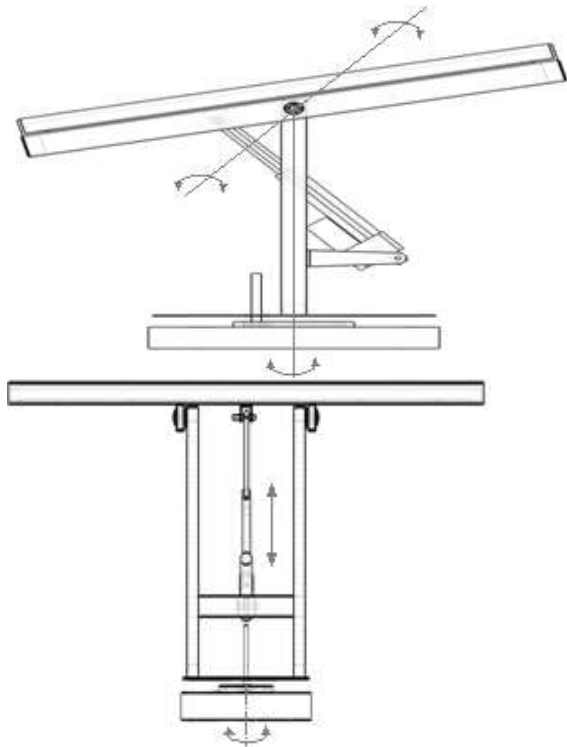


Fig. 12: Gear mechanism for motion of tracker base [10]

5 Free Body Diagrams (FBD)

Often used by physicists and engineers, free body is associated with the motion of a free body diagram, a pictorial device. In other words, when an object is kept independent from other objects for the purpose of dynamic or static analysis, it is considered to be "free". In the sense of being strained, the object does not have to be "free" and may or may not be in a state of equilibrium; rather it is not fixed in place and is therefore free to respond or react to the

forces and torques to which it is subjected. This situation is shown in Figure 13.



a-) Side view
b-) Front view

Fig. 13: 2 Dual axes and rotation

5.1 Panel

$$\sum F_x = R_{Ax} - R_{Ox} = 0 \rightarrow R_{Ox} = R_{Ax}$$

(4)

$$\sum F_y = R_{Ay} - R_{Oy} - W = 0 \rightarrow R_{Oy} = W - R_{Ay} \quad (5)$$

$$\begin{aligned} \sum M_O &= R_{Ay}(x - \delta) \sin \theta - R_{Ax}(x - \delta) \cos \theta = 0 \\ &\rightarrow \frac{R_{Ax}}{R_{Ay}} = \tan \theta \end{aligned} \quad (6)$$

This state, shown in Fig. 14.

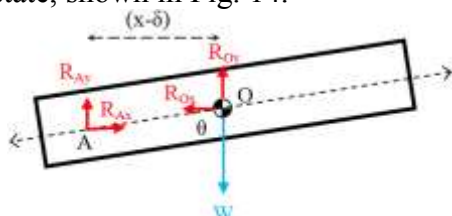


Fig. 14: Free Body Diagram of tracker panel

5.2 Linear Actuator

$$\sum F_x = R_{Ax} + R_{Bx} = 0 \rightarrow R_{Ax} = -R_{Bx}$$

(7)

$$\sum F_y = R_{Ay} - R_{By} + W_{la} = 0 \rightarrow R_{Ay} = R_{By} - W_{la} \quad (8)$$

$$\sum M_A = (x - a) W_{la} + y R_{Bx} - x R_{By} = 0$$

$$\begin{aligned} &\rightarrow R_{By} = \frac{(x-a) W_{la} + y R_{Bx}}{x} \rightarrow \\ R_{By} &= \frac{(x-a) W_{la} + y W_{la} \tan \theta}{x + y \tan \theta} \end{aligned} \quad (9)$$

This state, shown in Fig. 15.

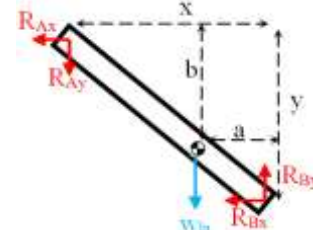


Fig. 15: Free Body Diagram of Linear Actuator

5.3 Vertical Beam

This state, shown in Fig. 16.

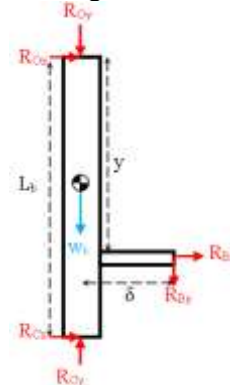


Fig. 16: Free Body Diagram of Vertical Beam

$$\sum F_x = R_{Ox} + R_{Cx} + R_{Bx} = 0 \rightarrow R_{Cx} = -R_{Ox} - R_{Bx} \quad (10)$$

$$\sum F_y = R_{Oy} + R_{By} + W_b - R_{Cy} = 0 \rightarrow R_{Cy} = R_{Oy} + R_{By} + W_b \quad (11)$$

$$\begin{aligned} \sum M_O &= -L_b R_{Cx} - y R_{Bx} + \delta R_{By} = 0 \rightarrow \\ R_{Cx} &= \frac{\delta R_{By} - y R_{Bx}}{L_b} \end{aligned} \quad (12)$$

5.4 Turn Table

The following conditions apply to the frame in the sun tracker system that makes the rotation horizontal and vertical.

1. All forces act in the same direction in a single plane.
2. Slight curvature at the ends, the smaller the tan, the smaller the section thickness, which appears almost straight lines.

3- Since the system is static, the force applied by the motor shaft on the turning table is zero and therefore it is not included in the analysis plane.

4- Depending on the variables z_b and D , the turning table will be subject to bending. The distance z_b will affect the stability and angular momentum of the functional model for dynamic motion. This situation is shown in Figure 17.

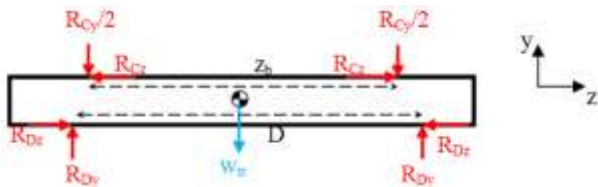


Fig. 17: Free Body Diagram of Turn Table (a)

$$\sum F_z = R_{Cz} - R_{Cz} + R_{Dz} - R_{Dz} = 0 \quad (13)$$

$$\sum F_y = R_{Cy} - 2R_{Dy} + W_{tt} = 0 \rightarrow R_{Dy} = \frac{R_{Cy} + W_{tt}}{2} \quad (14)$$

$$\begin{aligned} \sum M_C = \frac{z_b}{2} W_{tt} + \frac{z_b}{2} R_{Cy} + \frac{(D-z_b)}{2} R_{Dy} - \\ (z_b + \frac{D-z_b}{2}) R_{Dy} = 0 \rightarrow R_{Dy} = \frac{R_{Cy} + W_{tt}}{2} \end{aligned} \quad (15)$$

$$\sum M_C = 0 \quad (16)$$

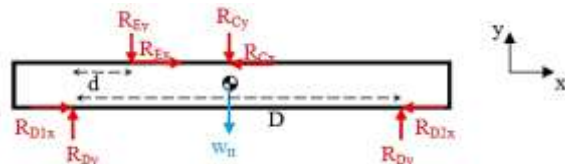


Fig. 17. Free Body Diagram of Turn Table (b)

$$\begin{aligned} \sum F_x = R_{Ex} - R_{Cx} + R_{D1x} - R_{D2x} = 0 \rightarrow \\ R_{Ex} = R_{Cx} - R_{D1x} + R_{D2x} \end{aligned} \quad (17)$$

$$\sum F_y = R_{Cy} - 2R_{Dy} + W_{tt} + R_{Ey} = 0 \rightarrow R_{Ey} = 2R_{Dy} - W_{tt} - R_{Cy} = 0 \quad (18)$$

$$\begin{aligned} \sum M_{D1} = DR_{Ey} + \frac{D}{2} W_{tt} + \frac{D}{2} R_{Cy} - DR_{Dy} + \\ tR_{Ex} - tR_{Cx} = 0 \end{aligned} \quad (19)$$

$$\rightarrow R_{D1x} = R_{D2x} = R_{Dx} \rightarrow R_{Ex} = R_{Cx}$$

5.5 Pinion Gear

The mating gears used here are Pinion and Big gears (Fig.12.) Mating gears work externally and internally. The difference between external and

internal running mates is that internally operating gears have different rotation directions in the input and output shafts. In externally operated gears, it has the same rotation direction in the input and output shafts. Fig.18. shows the forces on the pinion gear.

$$\sum F_x = R_{Fx} - R_{Ex} = 0 \rightarrow R_{Fx} = R_{Ex} \quad (20)$$

$$\begin{aligned} \sum F_y = R_{Fy} - R_{Ey} - W_p = 0 \rightarrow R_{Fy} = W_p - R_{Ey} = 0 \\ \rightarrow R_{Fy} = W_p \end{aligned} \quad (21)$$

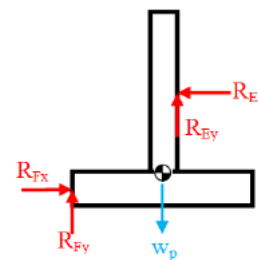


Fig. 18: Free Body Diagram of Pinion gear

5.6 Ball Bearing

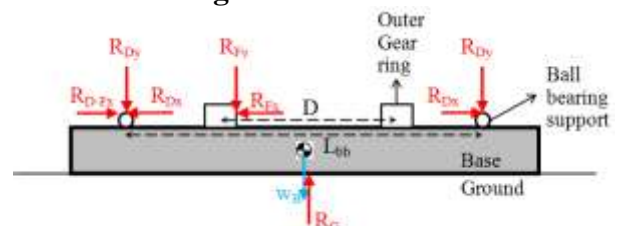


Fig. 19: Free Body Diagram of Pinion gear

$$\sum F_x = R_{Dx} - R_{Dx} - R_{Fx} = 0 \quad (22)$$

$$\begin{aligned} \sum F_y = 2R_{Dy} + W_B - R_G + R_{Fy} = 0 \rightarrow R_G = \\ 2R_{Dy} + W_B + R_{Fy} \end{aligned} \quad (23)$$

$$\rightarrow R_G = W + W_{tt} + W_{la} + W_p + W_b + W_B$$

For static analysis,

1. The center of mass of the linear actuator is approached 1/3 the distance.
2. All connections such as bolts, screws and nuts are assumed to have point contact.
3. All parts that make up the body of the audience are considered to be solid.
4. Parts mounted on the bodies are made of aluminum or steel material.
5. The linear actuator's center of gravity is assumed to be of negligible weight compared to the push rod's bulk portion of the linear actuator, [11].

6 Conclusion

In this study the dynamic behavior of a sun tracker mechanism was modeled and simulated using a commercial software package (20 sim). The functionality of the model was verified through the application of desired output criteria. According to the project plan, 2 dual axes design of sun tracker systems projects were successfully completed. The result of the 2 dual axes sun tracker design is suitable for the purpose of the project. As a result, an electro-hydraulic sun tracker was designed in the project. In the general section, the classification of the constructive structure, purpose and technical features of the sun tracker, and the designed tracker mechanism and working principle are explained. In the design section, rotation calculation is made in which the forces coming to the sun tracker supports and the dynamic forces arising in the system are calculated. 3D model was created in the solid works program. The aim of this project is to provide researchers with some skills and knowledge in this area after the project is completed. To teach the correct use of engineering mechanisms. Finally, the experience gained throughout this project is to help become a successful engineer in the future.

Reference:

- [1] Hongyu, T., Ziyi, Z. 2011. "Design and Simulation Based on Pro/E for a Hydraulic Lift Platform in Scissors Type," *Procedia Engineering* no. 16, p. 772-781.
- [2] Beer, F.P., Johnston, E.R., Eisenberg, E.R., Clausen, W.E. 2007. *Vector Mechanics for Engineers: Static & Dynamics*, ISBN 978-0-07-297698-4, McGraw-Hill, New York, USA.
- [3] Aksungur, Y., Nayir, M.Y., Güneş, E. 2012. *Senior Design Project: Design and Analysis of an Aerial Working Platform*, TOBB ETÜ, Ankara.
- [4] D. Karnopp, D. L. Margolis, and R. C. Rosenberg, *System Dynamics: Modeling and Simulation of Mechatronic Systems*, 4th ed. John Wiley and Sons, Inc., Hoboken, New Jersey, 2005. J. Clerk Maxwell, *A Treatise on Electricity and Magnetism*, 3rd ed., vol. 2. Oxford: Clarendon, 1892, pp.68-73.
- [5] C. S. Pan, A. Hoskin, M. McCann, D. Castillo, M. Lin and K. Fern, "Aerial Lift Fall Injuries: A surveillance and Evaluation Approach for Targeting Prevention Activities," *Journal of Safety Research*, Vol.

- 38, No. 6, 2007, pp. 617-625. doi:10.1016/j.jsr.2007.08.002
- [6] Rolland, L. 2010. *Kinematic Synthesis of a New Generation of Rapid Linear Actuator for High Velocity robotics*, *Advanced Strategies for Robot Manipulators*, S. Ehsan Shafiei (Ed.), ISBN: 978-307-099-5.
- [7] R. Sinha, V.-C. Liang, S. Member, C. J. J. Paredis, and P. K. Khosla, "Modeling and simulation methods for design of engineering systems," *Journal of Computing and Information Science in Engineering*, vol. 1, pp. 84–91, 2001.
- [8] L.W. Tsai, *Mechanism Design Enumeration of Kinematic Structures According to Function*. CRC Press LLC, 2001, ch. 9, p. 228.
- [9] Diaz-Calderon, C. J. J. Paredis, and P. K. Khosla, "Automatic generation of system-level dynamic equations for mechatronic systems," *Computer-Aided Design*, vol. 32, no. 5-6, pp. 339–354, 2000.
- [10] Geoff Rideout and Jeffrey L. Stein, "An Energy-Based Approach to Parameterizing Parasitic Elements for Eliminating Derivative Causality", *International Conference on Bond Graph Modeling (ICBGM' 2003)*.
- [11] *Solid Works Online Help*, Dassault Systèmes, 2014.

Creative Commons Attribution License 4.0 (Attribution 4.0 International, CC BY 4.0)

This article is published under the terms of the Creative Commons Attribution License 4.0 https://creativecommons.org/licenses/by/4.0/deed.en_US